GRANT NO: N00014-91-J-1232

FROM NORTH CAROLINA STATE UNIVERSITY
DEPARTMENT OF PHYSICS

FINAL REPORT FOR GRANT ENTITLED

CLUSTERS AND CLUSTER-ASSEMBLED MATERIALS

PERIOD OF PROPOSAL: 1 JANUARY 1991 - 31 DECEMBER 1991

PRINCIPAL INVESTIGATOR:
J. BERNHOLC, DEPARTMENT OF PHYSICS
NORTH CAROLINA STATE UNIVERSITY

DTIC
S **ELECTE**
JUN 0 5 1992
A **D**

North Carolina State University
Raleigh, NC 27695
IRS No. 56-6000-756
4th Congressional District

92 5 18 033

Review of Work To Date

Our work falls naturally into three categories: i) local density calculations of cluster structures and the development of classical potentials, (ii) simulations of thermodynamic properties of clusters and their fusion, and (iii) macroscopic (continuum theory) modeling of the sintering process. These topics will be addressed in turn. Although the nominal focus of the proposal is on sintering processes, many issues important to sintering are generic in nature and thus also important in other areas of cluster science. These issues have been approached from a broad perspective, leading to results which impact the whole field of clusters and cluster-assembled materials.

A. Local Density Calculations, Quantum Molecular Dynamics, and the Development of Classical Potentials

The objectives of the local density calculations and simulations are to i) obtain reliable information for the structure and energetics of small and medium size clusters; (ii) develop methods for first principles simulations of clusters; (iii) establish contact with the experimental community by calculating observables and comparing to the experimental data (cluster structures are not yet directly measurable); and (iv) develop potentials for long-time classical simulations of large clusters.

We have concentrated on Al, which is a "typical" free electron metal, and Cu, as a representative transition metal atom. For Al, we have carried out extensive Car-Parrinello and DVM calculations for clusters containing up to 55 atoms. Larger clusters, containing up to 2000 atoms, were studied quantum-mechanically using a jellium model. For Cu, DVM calculations for clusters containing up to 13 atoms have served as a basis for improving existing, efficient but very approximate "embedded atom method" (EAM) potentials. The results of the calculations

were used to interpret experimental data obtained by R. E. Smalley and R. L. Whetten, who are also participants in the ONR cluster initiative.

The quantum molecular dynamics part of this project was also supported by the Pittsburgh and the North Carolina Supercomputer Centers, whose Peer Review Boards have granted 541 and 120 hours, respectively, for the projects described below.

In our studies of the structures of Al clusters we have chosen to focus on large clusters, since the motivation for the present work is the study of clusters as building blocks for the production of cluster-assembled materials. Obviously, the structures of the clusters will play in an important role in the assembly process and thereby also influence the properties of the final material. The structural models most commonly used for metal clusters include fragments of bulk lattices as well as icosahedral structures.[1,2] Icosahedral structures are considered because they are believed to be the lowest energy structures for noble gas clusters up to very large cluster sizes.[3] Since metallic bonding is non-directional and results in highly coordinated structures, it has been widely believed that icosahedra are the ground state structures for metallic clusters. In particular, early theoretical calculations for atoms interacting with a spherically symmetric pair potential resulted in a prediction that the icosahedral structures will be preferred for up to ~ 2000 atoms.[4] However, Montano et al[1] concluded from the analysis of EXAFS data that 19-55 atom Cu clusters assume fcc structures. On the other hand, the authors of Ref. (2) concluded from the analysis of STEM data that Pd clusters smaller than 20 Å are icosahedral. These analyses suggest that this transition can occur much earlier for real metals and that its onset may strongly depend on the kind of atoms present in the cluster.

Our calculations for Al clusters were carried out using both the Car-Parrinello[5] and the DVM[6] methods. The current formulation of the Car-Parrinello method works most efficiently when plane waves are used as a basis set. This requires the use of periodic boundary conditions

A-1

and the clusters were embedded in a large simple cubic unit cell (ranging from 30 to 40 bohr, depending on the size of the cluster). Due to the size of our clusters we had to optimize the pseudopotential in order to obtain converged results with relatively small plane wave cutoffs. Tests have shown that the structural energy differences calculated here are well-converged with respect to both the supercell size and the cutoff.[7] The DVM calculations have used a numerical basis set consisting of the atomic core orbitals and the 3s, 3p, and 4s orbitals.[8]

The smallest clusters for which both perfect cuboctahedral and icosahedral structures exist contain 13, 19, and 55 atoms. The corresponding structures are shown in Fig. 1. Although the bulk interatomic distance is a good first-order guess for the interatomic distances in a cluster, the geometry clearly needs to be optimized. In the initial calculations we have considered the energetics of the two competing structures, allowing only breathing mode relaxations. In Fig. 2, the
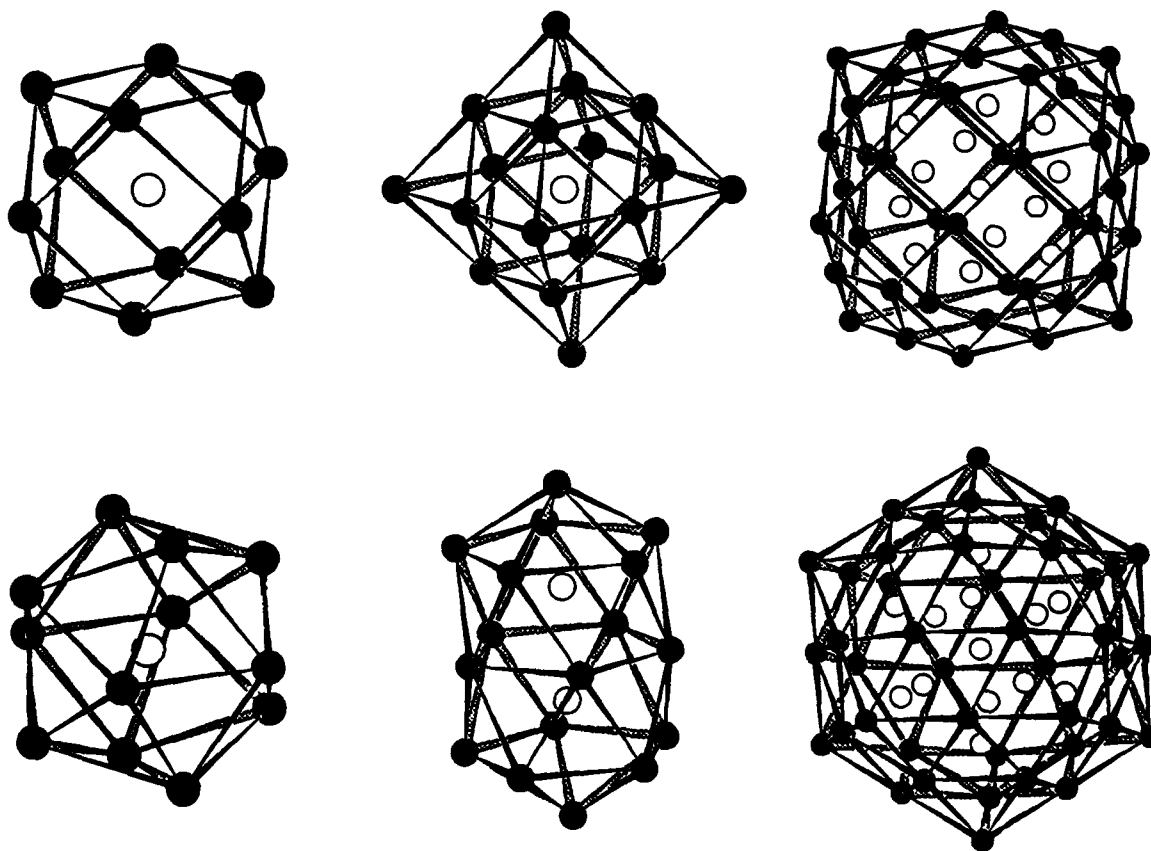

Fig. 1   The structures of the 13-, 19-, and 55-atom cuboctahedra and icosahedra.

binding energy difference between the icosahedral and the cuboctahedral structures is shown for two plane wave cutoffs: 4 and 6 Ry. It is evident from the figure that the icosahedron is preferred for the 13-atom cluster, but that the cuboctahedron is slightly preferred over the double icosahedron for the 19-atom cluster. For the 55-atom cluster, the energy difference between the cuboctahedron and the Mackay icosahedron increases, even on a per atom basis. DVM calculations carried out at the University of Chicago show also that the undistorted 13-atom icosahedron is more stable that the cuboctahedron and that this order reverses for the 55-atom clusters.[8]

These initial results thus predict a transformation to an fcc-based structure at ~ 55 atoms. In order to investigate this further we attempted to relax all the structural parameters of the 55-atom clusters using steepest descent and conjugate gradient algorithms without imposing symmetry constraints. For the icosahedral cluster, however, the rate of convergence of these methods was impractically slow. A slight heating of the cluster, which gave the atoms initial velocities, followed by a molecular dynamics relaxation with a friction term, found the minimum at a rate of 20-30 times quicker than the straight-forward minimization. This was due to the fact that the atoms largely kept their velocities during the relaxation, thereby traversing quickly through even
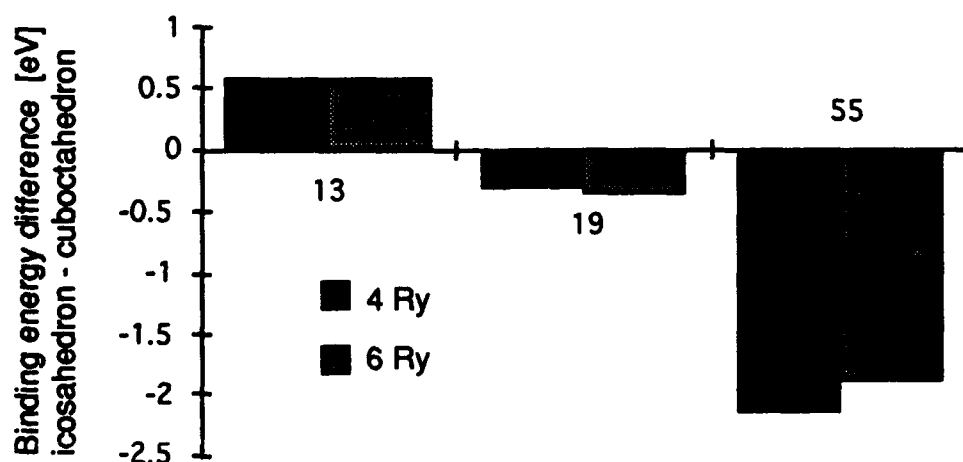

Fig. 2 The binding energy difference between the two alternative fully symmetric structures: the icosahedron and the cuboctahedron. Breathing mode relaxations are included.

Table I. Structural energy differences relative to the radially-relaxed Mackay icosahedron for the 55-atom Al cluster [eV/cluster]. The plane wave cutoff was 4 Ry (6 Ry).

	radially relaxed	"weakly-annealed"
icosahedron	0 (0)	-6.5
cuboctahedron	-2.1 (-1.9)	-5.3

the flatter parts of the potential energy surface.

The "weak annealing" procedure resulted in the reversal of the energies of the two structures, with the icosahedron now being preferred by over 1 eV over the cuboctahedron (see Table I). One should note, however, that since the energies of the two structures remained within ~ 1 eV, while the relaxation energies ranged from 3 to 6 eV, a search for a global minimum was necessary. Due to the size of these systems, however, this task was far from trivial. After considering several alternatives we adapted the efficient "constant thermodynamic speed annealing" method to molecular dynamics.[9] Our tests for a number of clusters have shown that this method is substantially more reliable than competing methods in finding the global minimum from a variety of starting configurations. In what is probably to date the largest quantum system studied by simulated annealing, we have succeeded in transforming an initially cuboctahedral 55-atom cluster to an icosahedron. Annealing of the icosahedron, on the other hand, does not change its structure. These results confirm that the "weakly-annealed" icosahedron is indeed the lowest energy structure for the 55-atom cluster. The energy difference between the icosahedral and the cuboctahedral structures is still unexpectedly small and appears dominated by surface reconstruction (see below). The transformation to fcc-based structures is thus still expected to occur very early for Al clusters.

Since the structure of small clusters cannot be measured directly at present and only indirect information is available, we set out to calculate Ionization Potentials (IPs) and Electron Affinities (EAs) for these clusters. This requires the evaluation of the total energy for charged states. However, the Car-Parrinello calculations proceed in supercell geometry and the energy of

a periodic array of charges diverges. Therefore, we had to develop special procedures for these calculations. We proceeded by carrying out CP supercell calculations for the charged clusters while adding a neutralizing background charge to the system. The neutralizing charge was spread uniformly throughout the entire cell and it had a very small effect on the total charge density. The CP charge density without the neutralizing background was used for the construction of the Coulomb potential for an *isolated* cluster, subject to zero boundary conditions at infinity. The whole procedure was tested by increasing the size of the cell, which lowers the density of the background charge and improves the treatment of the boundary conditions at infinity. The results were both stable and accurate.

The advantage of the present procedure for calculating IPs and EAs is that the plane wave basis set is used for the calculations of charged states. It has more variational freedom than atomic basis sets which are optimized for ground state calculations. The disadvantage is that the charge density used for the evaluation of the total energy of charged clusters is not strictly self-consistent. However, since the total energy expression is variational, this error is small, which is also demonstrated by the insensitivity of the results to the size of the CP cell (once it is sufficiently large).

The remaining errors in the calculations are due to the finite size of the basis set, the neglect of the spin polarization effects, and to the LDA. In order to further test the accuracy of our procedures as well as of the LDA, we calculated the ionization potential of the Al atom using the method described above (with the same plane wave cutoffs) and by numerically integrating the all-electron LDA equations with and without spin-polarization effects. The LDA all-electron result of 6.05 eV (including spin) is in excellent agreement with the experimental IP of 5.98 eV. Without spin-polarization, the all-electron result of 5.85 eV is in very good agreement with the CP value of 5.77 eV. The difference between the spin-polarized and the spin-averaged results can also be used as an estimate of the upper bound of the neglect of spin-polarization in our results

7

for clusters. We believe that these are the first high precision calculations of IPs and EAs for clusters.

The calculated and measured IPs and EAs are summarized in Table II. In comparing the calculated results to experiment, one should bear in mind that LDA is far more accurate in its predictions of IPs than EAs for small clusters. For large clusters the accuracy should be similar, since in the infinite cluster limit both the IP and the EA become equal to the work function, which is well predicted by the LDA. Table II also shows that the calculated results are higher than experiment by 0.4 – 1.0 eV. The experimental accuracy is better than 0.15 eV for the absolute values, while the differences between IPs or EAs for different cluster sizes are determined far more accurately. The discrepancies between theory and experiment are partially due to the use of the LDA approximation, in particular for the case of EAs, and partially due to the discrepancies between the calculated and measured structures. When the clusters undergo simulated an-

Table II. A comparison of the calculated and measured IPs and EAs for several cluster structures [eV]. The 1-atom case is treated as a test of the numerical accuracy of the Car-Parrinello calculations. See text.

	Calc IP		Exp IP	Calc EA		Exp EA
	CP	DVM		CP	DVM	
1-atom			5.98			
numerical LD	5.85					
numerical LD with spin	6.05					
Car-Parrinello	5.77					
3-atom cluster			6.42 - 6.45 *(a)*			1.5 *(b)*, 1.53 *(c)*
triangle	6.66			2.05		
13-atom cluster			~6.42 *(a)*			2.6 *(b)*, 2.86 *(c)*
icosahedron	7.15	6.0		3.81	2.9	
cuboctahedron	6.62			3.22		
annealed icosahedron	6.56			3.04		
19-atom cluster			5.60 *(d)*			2.85 *(b)*, 2.7 *(c)*
icosahedron	6.01			3.05		
cuboctahedron	5.81			2.81		
55-atom cluster			4.95 *(d)*			
icosahedron	5.10	5.15		2.87	3.2	
cuboctahedron	5.50	5.0		3.29	2.9	
annealed icosahedron	5.35			3.19		

(a) from Ref (10); *(b)* from Ref (11); *(c)* from Ref (12); *(d)* from Ref (13).

nealing, the agreement between theory and experiment improves substantially. For the larger clusters, structural differences for the unannealed structures are indeed the largest source of error (cf. Table II).

An analysis of the "weakly-annealed" structures (Fig. 3) has shown substantial differences as well as similarities. In particular, although the geometric structures are quite different, the structure factors and radial distribution functions are very similar. These results cast substantial doubt on the value of line shape analysis of scattering data as a tool for the determination of the structure of small particles. Although not very apparent from the figure, the changes in the core of the clusters upon annealing are small and most of the atomic rearrangement occurs on the surface, as expected.

The analysis of the Al clusters can be carried much further by considering the structure factors, angular distributions, and pair correlation factors for the ideal, weakly annealed, and fully annealed structures. An interesting aspect of annealing studies which can be afforded on to-day's supercomputers is that each QMD run results in a significantly different structure.[14] An analysis based on the structure factors and distribution functions shows[14] that the local topology of each structure is almost the same, i.e., the nearest neighbor and the most probable angle peaks occur at exactly the same positions for the three annealed clusters, and there are strong similarities in the positions of second neighbor peaks. It follows that the energetics of Al_{55} is mainly determined by the first and possibly second nearest neighbors. This result provides a justification for the success of the effective medium and embedded atom methods,[15] in which the screened interatomic interactions in metals are approximated by short range effective potentials.

The multitude of structures for the 55-atom cluster is possible because most of the atoms reside on the surface and are therefore free from the constraints of bulk packing. Due to the size of this cluster, slight changes in the positions of distant neighbors can lead to completely in-

9

equivalent structures. However, a careful analysis of the annealed structures on graphics work-stations capable of manipulating three-dimensional images shows that the positions of the inner atoms differ substantially between these structures so that the clusters cannot simply be modeled as a common core and differently arranged surfaces.

We have also carried out a number of Car-Parrinello calculations in order to establish a library of structure-energy relationships for the fitting of classical potentials. When these results were compared to those obtained using a bulk EAM potential, we found that although the amount of radial relaxation was predicted very well for a *given* geometry, the energy differences between different structures were predicted less well, and sometimes resulted in a wrong order-ing of the structures (Fig. 4). We have considered several schemes for the development of a po-tential specifically fitted to clusters. The method which worked best to date, however, involved just fitting the values of the embedding function and its derivative to the results of quantum-me-chanical calculations for the equilibrium structures of clusters consisting of 3-12 atoms. This procedure resulted in a better determination of the embedding function in the region of small densities, without sacrificing the bulk region. The improvement in the results for the 13- and 19-atom clusters in both the icosahedral and the cuboctahedral geometries was substantial. However, the improved embedding function still predicted the ideal icosahedron to be lower in energy than
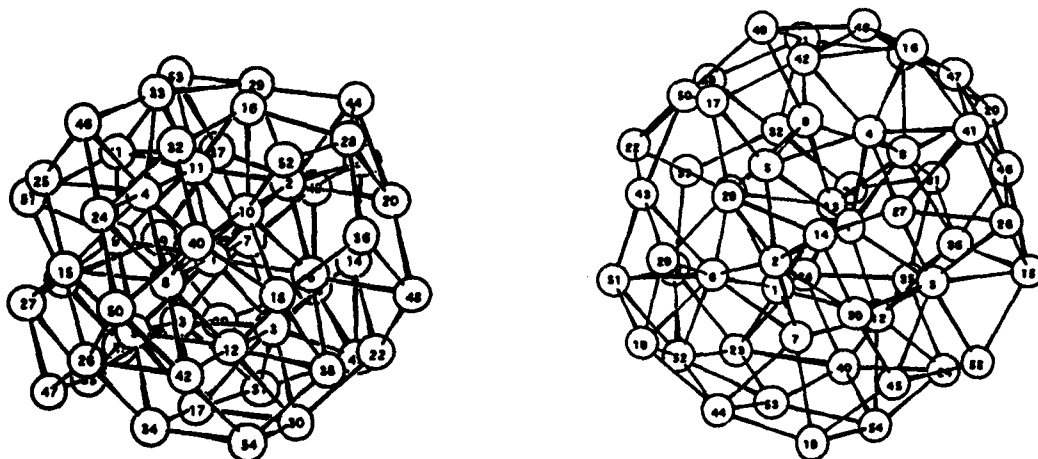

Fig. 3. The structures of the weakly-annealed cuboctahedron and icosahedron.

10

the cuboctahedron. Including the 55-atom clusters in the fit resulted in a correct ordering of the structures (see Fig. 4).

Several points should be made about the EAM results to date: (i) Although small clusters were used in the fit, only modest improvements are seen in the 3-8 atom cluster range. This is most likely due to the fact that the quantum effects are the strongest in this range, due to the large spacing between the energy levels in small clusters. When this spacing decreases, the EAM description should get better. For cluster sizes greater than 12, the improvement is substantial; (ii) The fitting of the 55-atom results has resulted in a variation of the curvature of the embedding function, although the function .tself has remained monotonic; and (iii) The distorted geometries resulting from energy minimization in the quantum-mechanical calculations lead to an increase in the EAM total energy even when the improved embedding function is used. Due to the complexity of the potential energy surfaces uncovered by the Car-Parrinello calculations, we believe that further improvements in this potential are needed.

For clusters larger than ~ 100 inequivalent atoms even the fastest methods for quantum-mechanical calculations for clusters become too expensive. However, spheroidal clusters containing thousands of atoms can still be studied utilizing a jellium approximation, which is
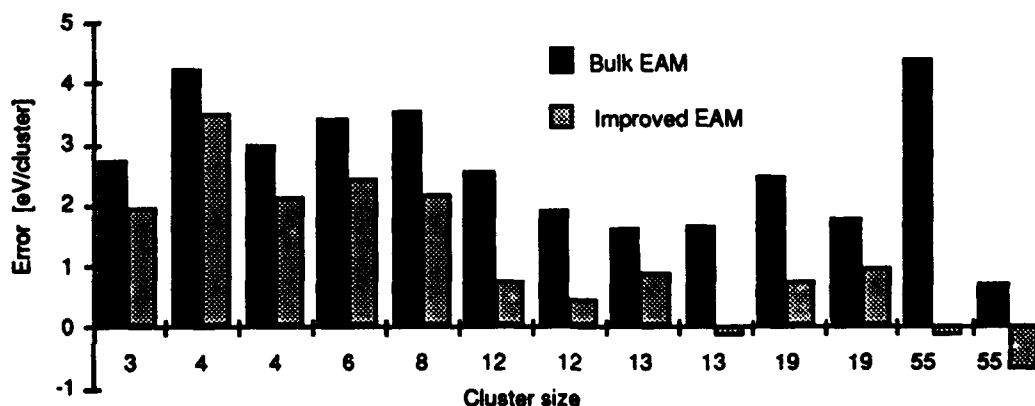

Fig. 4. The difference between the quantum-mechanical and EAM results, using the bulk Al EAM potential and the cluster-derived (improved) EAM potential.

11

known to work very well for bulk Al. Indeed, the work described above has shown that the structural changes occur mainly at the surface, and in very large clusters inner atoms out-number surface atoms by a substantial margin. Our jellium calculations have been carried out for clusters containing up to 2000 atoms, and found that they exhibit groupings of electronic energy levels into what have been called supershells.[16] Such groupings have been seen in the experiments of our collaborator, R. L. Whetten. In contrast to the levels of the large clusters, we have found by comparison to results of our DVM calculations[8] that the jellium model does not represent well the electronic level structure of smaller clusters, e.g. Al_{55}. The size, boundary effects and effective crystal field together cause the level pattern to deviate strongly from the pattern implied by the jellium model. The convergence to jellium-like behavior may become a useful index of the extent of metal-like behavior in small clusters.

We have also initiated the construction of an embedded atom[15] Cu potential for clusters, utilizing previous EAM results as well as our DVM calculations for several structures of Cu_6, Cu_9, and Cu_{13}. Our strategy here is to adjust the parameters of the simple potentials to fit results of local density calculations in the vicinity of the most important points on the multidimensional potential surface, namely minima and saddle points. This procedure is now feasible because locating saddle points is now almost as easy as locating minima.[17] To date,[18] the adjustments of the embedded atom potential have only been made in the regions of the secondary minima, and not yet in the regions of the saddle points. However, the feasibility of the method has been established and its full implementation is one of the tasks for our next phase.

Although the Car-Parrinello method is quite general, its most efficient implementation relies on the use of a plane wave basis set. Periodic boundary conditions are necessarily imposed, and calculations involving first-row or transition metal atoms become quite expensive, sometimes prohibitively so. In order to reduce the computational effort for such clusters, we have developed a new real space method based on multigrid techniques which can be used with or with-

out periodic boundary conditions. It can also handle first-row and transition metal atoms without a substantial increase in computational time. In this method, the Kohn-Sham and Poisson's equations are solved on several grids at a time. The final solution is obtained on a sufficiently fine grid so that it represents well the pseudo-wavefunctions and the pseudopotentials in the problem. However, the convergence is accelerated by the use of several auxiliary grids, each with the spacing increased by a factor of two over the previous grid. Denoting the grid spacing by Δx, one can show that iterations on any given grid reduce quickly those Fourier components of the error with wavelengths $\sim \Delta x$ but are ineffective when dealing with substantially longer wavelengths. The role of the extra grids is thus to converge quickly and systematically *all* wavelength components of the error. One important advantage of the algorithm is that the grids need not be uniformly spaced so that the grids can be enhanced locally near, *e.g.*, transition metal atoms. Substantial programming and some algorithm development efforts are still needed, but we already obtained test results for H, H_2, Li, and LiH. Some of these results have been described in invited talks at the Faraday's bicentennial[19] and the cluster conference in Richmond.[20]

A major new effort initiated under this grant and continued in a separate grant is a study of buckyballs and related structures. Under this grant, we computed the equilibrium atomic structure of solid C_{60} and studied its dynamics during heating to high temperatures.[21] The calculations determined the precise atomic positions of the carbon atoms (which were much later confirmed by neutron scattering), showed that C_{60} start to rotate at relatively low temperatures even when in a solid form (which explained NMR data), and that they are stable even at very high temperatures. These results received a very wide exposure and were quoted in several scientific and popular periodicals. The electron distribution figures and snapshots from the QMD simulations have appeared on the covers of Science News, Science, Scientific & Engineering Indicators 1992, and in several books and foreign periodicals.

B. Classical Molecular Dynamics Simulations

Our simulations have focused on the issues associated with melting and surface melting of clusters, which have important consequences for cluster fusion and sintering; on modeling of cluster fusion; and on the development of an analytical quantum-statistical theory of surface melting. The last project has been to a large extent guided by the results of the simulations, which is the reason for its inclusion into this section. As in the case of our quantum calculations, the issues have been approached from broad perspective, resulting in generic results with wide applicability.

The simulations of single clusters have shown that clusters of fewer than about 45 atoms show no behavior that could be called surface melting. Instead, some display simple melting, and others show softening, manifested by passage among a limited set of catchment basins on the cluster's multidimensional surface, and then, at higher energies, a transition to liquid-like behavior. This means that "liquid-phase sintering", the process by which the necks of sintering particles are filled by liquid-like, mobile material, is a concept applicable to clusters containing two or more shells of atoms. However for clusters of about 50 or more atoms, surface melting seems to be the general rule, occurring over a range of temperatures well below the bulk melting temperature. Figure 5 illustrates the diffusion coefficients in melted surfaces, as functions of the mean cluster temperature, for Lennard-Jones clusters of four sizes.

The criteria for surface melting are the same as those for bulk melting of clusters, but can be applied only by designating the particles in the cluster's surface to be distinguishable from those in the core of the cluster. Making this distinction is straightforward to incorporate into simulations by classical mechanical molecular dynamics (MD), the procedure we have used for most of the simulations for this work. These criteria include: the "Lindemann criterion" of large-amplitude motions of nearest neighbors, meaning 10% or more of the equilibrium interparticle dis-

tance; diffusion, typically evaluated from the mean square displacement of the atoms from their initial locations, as functions of time, (which is a necessary but not sufficient condition for liquid-like behavior); the occurrence of vibrational modes of very low frequency ("soft modes", also a necessary but not sufficient condition); passage of the system among many potential wells at a rate not very different from the frequency of vibrations within one well, which is probably both necessary and sufficient if the set of wells visited includes those of permutational isomers of the structure of lowest energy; and passage among *all* the permutational isomers of the structure of lowest energy, which is a sufficient but not a necessary condition for liquid-like behavior. There are others, such as pair or radial distribution functions and angular distribution functions (which give necessary but not sufficient conditions for liquid-like behavior because amorphous solids look like liquids according to these criteria), which we also sometimes use.
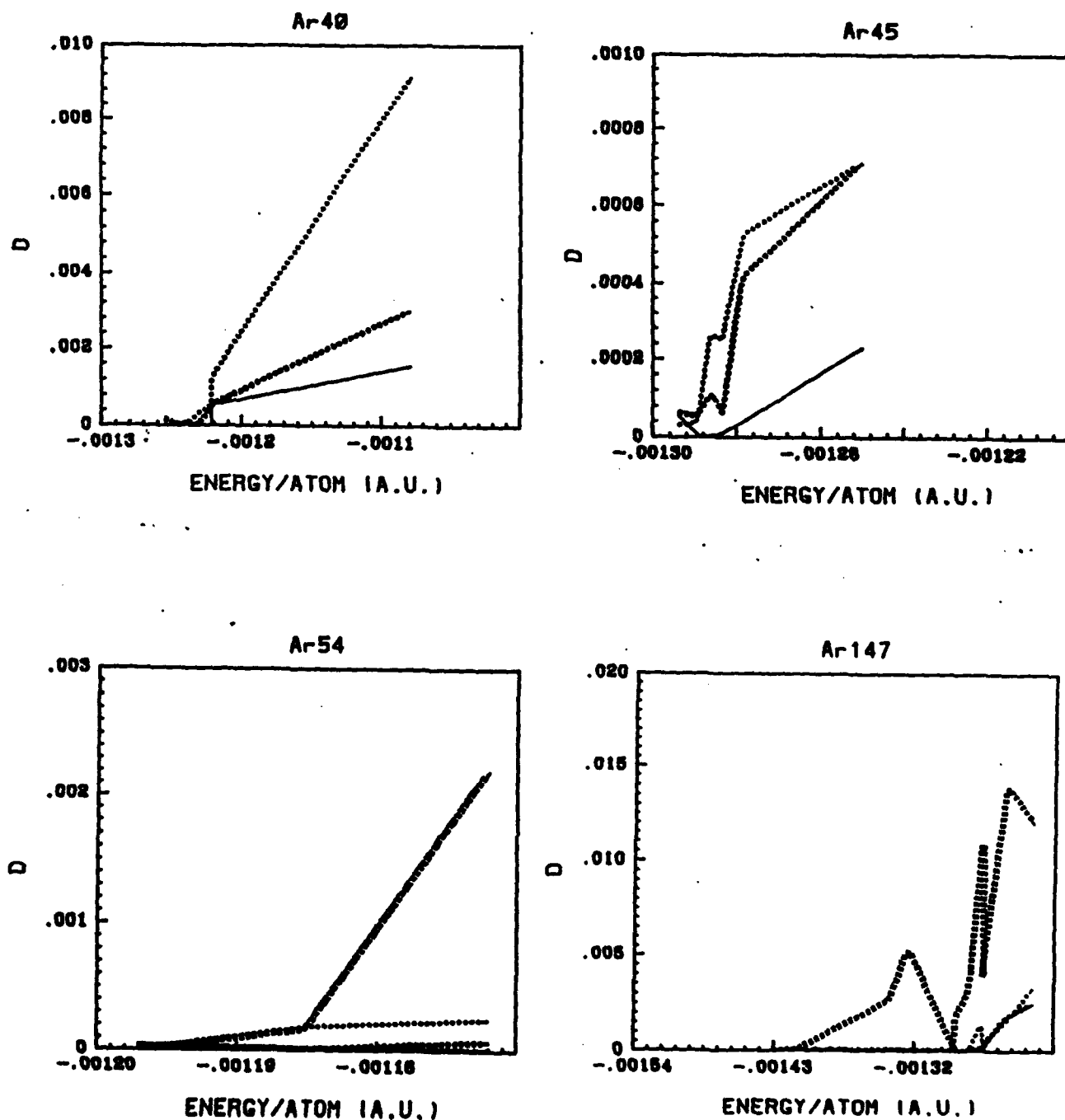
Ar-40

Ar-45

Ar-54

Ar-147

Fig. 5. Temperature and size dependence of the diffusion coefficients for Lennard-Jones clusters with liquid-like surfaces.
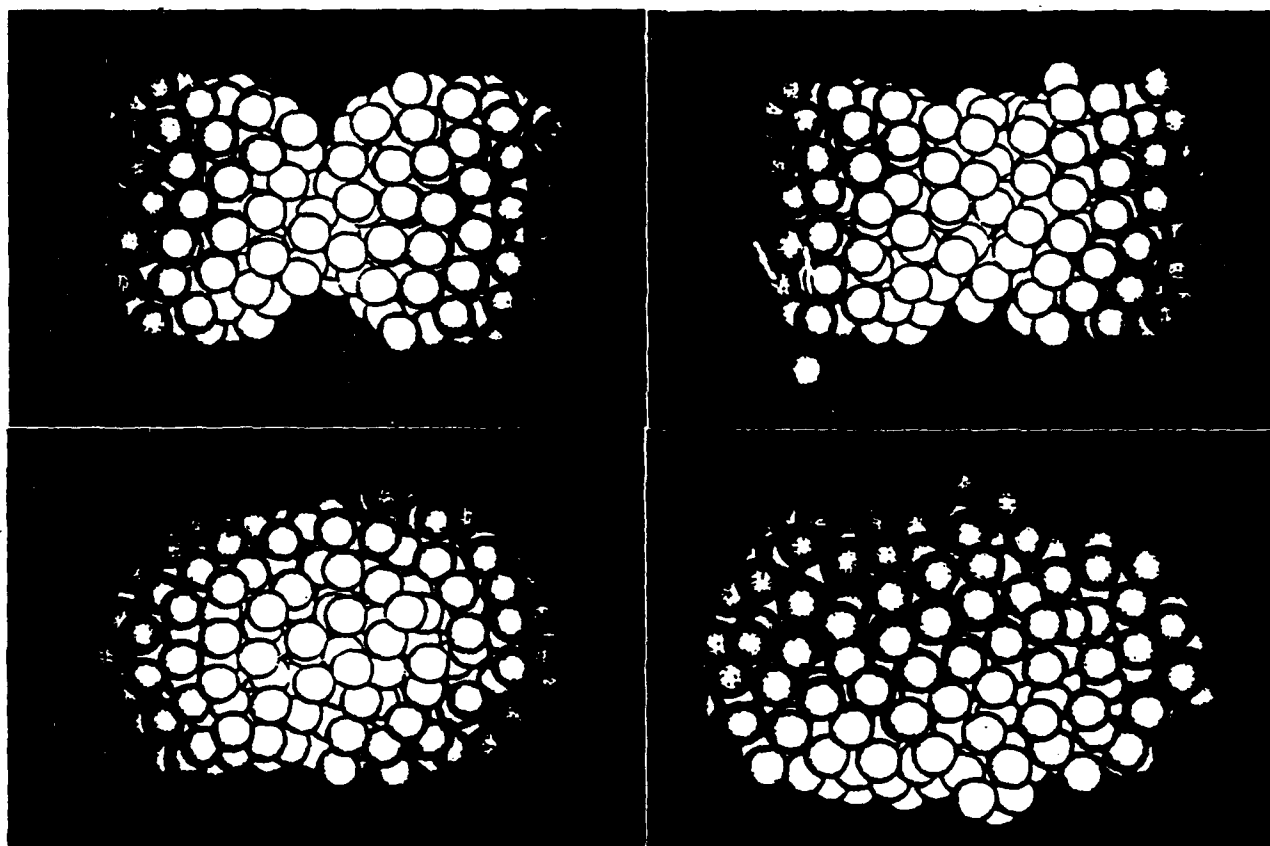
16

Fig. 6. Examples of snapshots of two $(Ar)_{147}$ clusters during the process of sintering: a) after 1000 steps of 10^{-15} sec; b) after 10,000 steps; c) after 40,000 steps; d) after 100,000 steps.

Simulations of Lennard-Jones clusters ranging in size from 45 to 147 atoms have provided diffusion coefficients for these clusters as functions both of temperature and of cluster size. Examples are shown in Fig. 5. While the diffusion coefficients for clusters of fixed size are smooth functions of temperature, they are not smooth functions of cluster size, at least in the lower end of our size range. It will be necessary, in order to make the general theory readily applicable to clusters of all important sizes for sintering, to carry the simulations of surface melting to clusters large enough that the size dependence of the diffusion coefficient is smooth. This will be a direct continuation of work already done, and will not be particularly demanding, although a substantial amount of computer time will be needed.

The simulation of sintering itself has been carried out for pairs of Lennard-Jones clusters of 147 atoms. Such clusters exhibit a combination of liquid-phase sintering and reconstruction which allows an approximate separation of the process into an early stage of neck formation and a second stage of cementing and reconstruction, during which the two clusters still retain some visible identity. Copies of photographs of some of the computer animations of these simulations are shown in Fig. 6.

Simulations of surface melting on single clusters of 147 argon (Lennard-Jones) atoms revealed unforeseen characteristics of that process. Individual frames showing the cluster at arbitrary instants along its MD trajectory fit our prior expectations; the core of 55 atoms retains its identity as a polyhedron with only small-amplitude distortions but the atoms of the surface seem to be amorphous, with no obvious polyhedral structure. However, movies of the same simulations show that the real situation is not just the formation of a liquid layer around a solid. In the energy range within which the diagnostics say that the surface is molten and the core is solid, the situation is rich and complex. Most of the core atoms, in any brief time interval, execute large-amplitude, anharmonic oscillations about equilibrium positions on the polyhedron of the solid cluster, while one or a few atoms play the role of "floaters", moving rather easily around the surface of the cluster. Over time, the "floaters" exchange roles with the other atoms of the surface layer, so that permutations and diffusion are achieved. The set of surface atoms meets all the criteria of liquid-like behavior, but by microscopic means quite different from what was traditionally expected of liquids. On this basis it is important to reexamine the thermodynamic analysis of surface melting of clusters, which had previously implied that liquid surfaces of clusters are stable only as fluctuations of thermally equilibrated solid clusters.[22]

To give a basis to the simulations of surface melting, we developed an analytic, microscopic quantum-statistical theory of surface melting. This is parallel, in some ways, to the theory we developed for homogeneous melting of clusters,[23-25] but has a different form precisely be-

cause of what we have learned about "floaters" and "stay-at-homes" from the simulation movies. A combination of simulation and analytic, statistical-mechanical theory led to a new, quantifiable model for surface melting of clusters and to a set of diffusion coefficients for clusters of various sizes at various temperatures. A full report of this work in now in press.[26] The conclusions of this work are that surface melting of clusters of atoms bound by central forces is a real phenomenon for clusters of more than about 50 atoms, that the mechanism of this melting is primarily the promotion of a few surface atoms from the outer shell to a "floating" state outside the normal outermost shell, leaving a vacancy there, that most of the diffusive motion is carried by the "floaters" which exchange occasionally with atoms in the surface layer, that the surface-melting transition has only a single stable form at any temperature and pressure and is in this sense like a second-order phase transition rather than a first-order transition (as homogeneous melting of clusters is), and that because the process involves formation of floaters, it has a small latent heat and is therefore not a true second-order phase transition.

A second achievement of this group was the development, in collaboration with Professor Robert Whetten and his student Xiuling Li, of a full phase diagram for a cluster. (Professor Whetten's work is being carried out under the same ONR Initiative as our own.) This is the first time that full diagrams of the curves of equal mean chemical potential, in terms of pressure and volume, pressure and temperature, and volume and temperature, as well as heat capacity and thermal expansion coefficients, have been developed for a realistic cluster of atoms. This work is now in press[27] and is also being presented at the Spring Meeting of the Materials Research Society in San Francisco, 1992.

In order to address nonmetallic clusters relevant to real applications, particularly to sintering of refractory powders, we have investigated the behavior of salt clusters, particularly $(KCl)_n$. These were chosen because they can be modeled reliably and are similar in many ways to metal oxide clusters, which are of obvious general interest. Clusters of NaCl have been studied for a

variety of reasons,[28,29] but not for the purposes we followed: surface melting, the possibility of glass formation and, ultimately, sintering. The results to date have not yet given a clear answer about surface melting, largely because we have not yet simulated clusters large enough to be expected to show that phenomenon. The results regarding glass formation are striking: it appears that clusters as small as $(KCl)_{16}$ are capable of being quenched to glasses.[30] The stability of these glasses is not yet known, and will be one of the most important questions to be addressed in the future. Bulk ionic glasses have been recognized for some time.[31,32]

C. Continuum Modeling

The continuum theory part has achieved several of its initial goals. We have developed an analytic theory of the shapes of sintering bodies in first-stage sintering,[33, 34, 35, 36] a quantitative theory of the unpinning and elimination of grain boundaries in sintering[37], and a quantitative theory of third stage sintering[38]. In the arena of simulations, an intensive database of random close packed structures of distributions of sphere sizes has been amassed and used to report and model the statistics of contact distributions[39]. These distributions were used to simulate early stage sintering to study the relative effects of grain boundary versus surface transport[40, 41]. The computations associated with this part of the effort amounted to over 500 Cray hours. This time was provided by San Diego Supercomputer Center via a block grant to SDSU.

Since the driving force for sintering is the reduction in surface and grain boundary areas during particle fusion, our study of macroscopic models began with the observation that the static geometric structure of the sinter, representing the solid skeleton and the mobile pool, may be characterized as a new version of the problem of minimal surfaces: Plateau's problem. The new version follows simply from the exotic nature of the "liquid" pool which covers the solid skeleton. The exoticness of this liquid derives from the near indistinguishability of the solid and liquid forms making the surface tension between liquid and solid zero and the surface tensions of vapor

against solid or vapor against liquid equal. Furthermore, microscopic pore sizes make gravitational effects negligible. This leaves us with a much simplified special case of the classical theory of capillarity. This case was considered unphysical and left by the wayside by previous generations of mathematicians and physicists. It is however, the physically appropriate model for sintering processes. This discovery has already lead to some interesting developments in capillarity and in understanding the geometry of microporous materials and is certain to lead to many more. It turns out that the special case lends itself to a different mathematical formulation[33] which is much more amenable to analytic attack. This allowed us to construct nearly analytic solutions for the early stages of sintering.[34,33] It also allowed us to prove such theorems as: The mean curvature on a solid portion of the skeleton surface is everywhere greater than the mean curvature of the liquid portion. Perhaps most importantly, it promises a universality of structure among pores found in sinters. Our formulation of the generalized Plateau problem represents an important spinoff application that this project has produced for the theory of minimal surfaces. The generalized problem leads naturally to several other interesting new problems in the theory of minimal surfaces[42].

Our analysis beyond the static structure has leaned heavily on the assumption that the rate limiting step for the sintering process is the creation of a mobile pool of material. For convenience, this pool will be called "liquid" below although the only requirement in the formalism is that the mobility of this pool be much greater than the diffusion rate of the atoms in the core. The latter assumption has been shown to hold by microscopic simulations (see preceding subsection). As a consequence of this assumption, the redistribution of the "liquid" will lead to an equilibrium configuration that minimizes the surface area, which is proportional to the free energy of the system. The local mean curvature represents a generalized force responsible for the motion of the mobile pool. It follows that the mean curvature of any optimal surface is constant wherever it is covered by the mobile pool, since such surfaces represent equilibrium configurations.

The generation of optimal surfaces did not turn out to be straightforward however. We began with the case of two identical solid spherical particles in point contact, wetted by a certain volume of liquid. The assumption of spherical particles is mild since any spheroidal shaped particles become spherical once a mobile pool of atoms is created. The situation for identical two spheres was described by a first order differential equation, which turned out to be singular in an important region of the parameter space. Schemes were found for stabilizing the singularity and the equation was finally solved by numerical integration. The integrand contained two Lagrange parameters whose values had to be matched by shooting methods. An overlap parameter was added which (if negative) could also describe the case of separated spheres. The generated solutions could simulate the sintering of two spheres and of a close packed configuration of spheres with any desired ratio of surface to grain boundary melting. Furthermore, these simulations evolved the solid skeleton as well as the mobile liquid pool and thus went far beyond the original solutions of the static case. The results for two identical spheres were published in Ref. (34) where it was seen that in some cases significant differences existed between the shapes calculated by minimizing the free energy and the shapes assumed by previous workers.

The simulations above used our analytic and numerical work on the problem of unequal spheres. New methods were developed including an explicit algorithm for the construction of the minimal surfaces needed to solve the sintered shape problem in any axially symmetric case.[35,36] We noted there that the problem is fundamentally combinatorial in nature with many cases determined by the geometry of the solid to be wetted. We showed that these cases could be conveniently handled by noting the volumes of certain "separatrix" solutions, which restrict the range of choices for the boundary conditions. The identification of these separatrix solutions is important for maintaining stability and convergence properties of the algorithms.

The global problem of minimizing the free energy by optimally allocating the liquid among the puddles is again a difficult combinatorial optimization problem. Our discovery, that it is pos-

sible to map this problem into a dynamic programming problem[40] is an important innovation both for the simulations in this study and the understanding of microporous geometry.

For unequal spheres, the first observation was that the point of minimal constriction between two unequal size spheres moves in response to the force to maintain the smallest possible surface area as liquid is added. Once the constriction between the spheres disappears, the grain boundary becomes unpinned and anneals out. We have carried out essentially exact simulations of grain boundary annealing. The first surprise was that the unpinning always occurs when the liquid neck between the two spheres is exactly tangent to the top of the smaller sphere. The second surprise was that the thinnest point in the neck does not necessarily move directly toward this point; its initial movement is toward the center of the larger sphere, provided that grain boundary transport is fast compared to surface transport, i.e. the primary source of the mobile pool is the grain boundary.[37]

Generating the solutions for unequal size spheres in terms of the physically important variables such as liquid volume and sphere-sphere overlap (rather than the Lagrange parameters) turned out to be also a numerically demanding problem. In order to simplify most of the time evolution runs we decided to create a database of solutions suitable for splining. This data base was assembled and will prove invaluable for the continuing work:

Database 1: Numerical solutions of the shapes (and all geometric parameters) of the optimal surfaces required to describe the wetting of two spheres of radii r_1 and r_2 with separation h using an amount V_L of liquid volume.[36,35] Using this information we can give a complete description of the evolution of two solid spherical particles for any ratio of surface/grain boundary transport.[35] Furthermore, the comparison between neighboring optimal surfaces for infinitesimal changes in the arrangement of the solid skeleton gives the forces acting on the solid cores of the

particles. The solutions thus provide nearly the complete information necessary for simulating the time evolution of the structure of the sinter.

Our next concern was to start with a reasonably accurate model of the sinter. Accordingly, we generated a second database:

Database 2: Configurations of random packed spheres and disks with various distributions of radii.[39] This data base has provided statistics for modeling the distribution of sphere-sphere contacts. It also provides the initial configurations for simulating sintering processes.

The simplest model for time-evolution of the sinter uses the random packings in database 2 to provide the number and type of sphere-sphere contacts and evolves these independently employing the information stored in database 1. This is a direct application of the methods in Ref. (34) for a distribution of sphere sizes and necks. We have also explored versions of this model which allow partial interaction between neighboring necks by allocating mobile volume among the necks in an optimal fashion.[43]

While such models give qualitatively useful information -- see Amar et al.[34] for the case of identical spheres and Schön et al.[40, 41] for the case of a random close packed array of spheres -- they neglect the change with time of the three dimensional structure of the solid material beyond the independent pairs approximation. They also neglect the possible coalescence of neighboring necks.

The work described above deals with early stage sintering; we have also had good success in late stage sintering. Following standard usage, we distinguish three different stages of the sintering process.[44] During first stage sintering, the mobile material forms bridges between neighboring sintering particles, and fills in narrow necks. During second stage sintering, the channels

that connect various regions of the sinter close, creating weakly connected pores in the process. These pores will become approximately spherical at the conclusion of this stage. Finally, in the third stage, the pores exchange material via connecting grain boundaries, leading to growth of ₋ne bigger pores at the expense of the smaller ones; this is the so-called coarsening process.

For third stage sintering the situation is simple enough for an analytic attack. We have modeled the third stage as a coarsening process of the Lifshitz-Slyozov type[45] that proceeds via grain boundary diffusion.[38] The slow time scale is still the promotion of a particle to the "mobile pool," but in this case the mobile pool is just the material in the grain boundary connecting different spherical pores. Since the distances between the isolated pores are large, each pore effectively equilibrates with the reservoir of material in the grain boundaries, which in turn serves as the medium for the interaction among the pores leading to a growth of the larger pores at the expense of the ⁻maller ones. Thus far we are dealing with the standard Lifshitz-Slyozov model.[45] The distinction comes in observing that the grain boundary represents only a two dimensional medium coupling our three dimensional pores. We solved the Lifshitz-Slyozov model[45] for the case of an m dimensional medium surrounding n dimensional pores.[38] The specific example of m=2, n=3 was treated in detail to deduce the time evolution of the size distribution of pores connected by grain boundaries, as well of the average pore size and the number of pores per unit
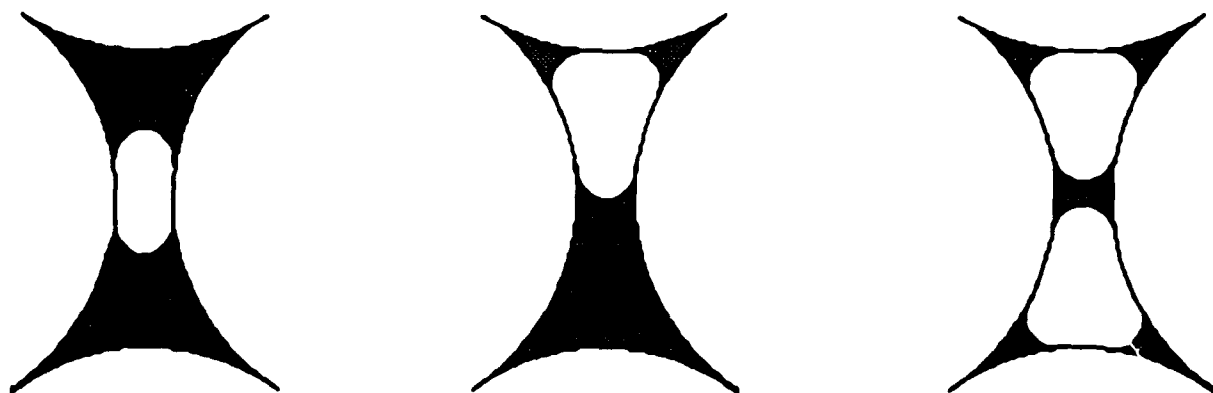

Fig. 7. Three competing equilibrium structures for filling a pore between four identical disks.

volume.

The problem of second stage sintering is much more difficult to simulate. The reason is already evident in two dimensions, where much more is accessible analytically. As an illustration, consider a pore between four identical disks. This simple case already reveals an unexpected complexity of structure[46] with three competing local minima: symmetric, asymmetric, and bridged (see Fig. 7). Each of these types represents the energetically favored configuration over some range of the area parameter.

Even ignoring the problems due to local minima such as these, the interaction between necks presents several new difficulties, which are common to both the two- and three-dimensional case. They are associated with keeping track of which necks have coalesced and how to classify, lookup, and calculate the associated "many-neck" puddles. Since we are able to investigate these issues more easily for two dimensional sintering, we plan to begin exploring second stage sintering by implementing the simulation in two dimensions. The program and associated data structures handle two or three dimensional problems with equal ease so the transition to three dimensional data is anticipated to be relatively easy. The two dimensional case will develop the necessary intuition for modeling the more involved three-dimensional case. It is also expected to reveal the appropriate universality classes of pore structures in two dimensions. The transition to three dimensions can be achieved using the Surface Evolver package developed by the Minnesota Supercomputer Center. Preliminary work implementing this software has shown that it is capable of the task. The calculation for three spheres is presently being generated.

References

1. P. A. Montano, G. K. Shenoy, E. E. Alp, W. Schulze, and J. Urban, Phys. Rev. Lett. **56**, 2076 (1986).

2. H. Poppa, R. D. Moorhead, and M. Avalos-Borja, J. Vac. Sci. Technol. A **7**, 2882 (1989).

3. J. C. Phillips, Chem. Rev. **86**, 619 (1986).

4. J. G. Allpress and J. V. Sanders, Aust. J. Phys. **23**, 23 (1970).

5. R. Car and M. Parrinello, Phys. Rev. Lett. **55**, 2471 (1985).

6. E. J. Baerends, D. E. Ellis and P. Ros, Chem. Phys. **2**, 41 (1973); B. Delley, D. E. Ellis, A. J. Freeman, E. J. Baerends and D. Post, Phys. Rev. B **27**, 2132 (1983).

7. J.-Y. Yi, D. Oh, J. Bernholc, and R. Car, Chem. Phys. Lett. **174**, 461 (1990).

8 H.-P. Cheng, R. S. Berry and R. L. Whetten, Phys. Rev. B **43**, 10647-53 (1991).

9. J.-Y. Yi, J. Bernholc, and P. Salamon, Comp. Phys. Comm., **66**, 177 (1991).

10. D. M. Cox, D. J. Trevor, R. L. Whetten, and A. Kaldor, J. Phys. Chem. **92**, 421 (1988).

11. G. Ganteför, M. Gausa, K. H. Meiwes-Broer, and H. O. Lutz, Z. Phys. D **9**, 253 (1988).

12. K. J. Taylor, C. L. Pettiette, M. J. Craycraft, O. Chesnovsky, and R. E. Smalley, Chem. Phys. Lett. **182**, 347 (1988).

13. K. E. Schriver, J. L. Persson, E.C. Honea, and R. L. Whetten, Phys. Rev. Lett. **64**, 2539 (1990).

14. J.-Y. Yi, D. J. Oh, and J. Bernholc, Phys. Rev. Lett. **67**, 1594 (1991).

15. J. K. Nørskov, Phys. Rev. B **26**, 2875 (1982); M. S. Daw and M. I. Baskes, Phys. Rev. B **29**, 6443 (1984); S. M. Foiles, M. I. Baskes and M. S. Daw, Phys. Rev. B **33**, 7983 (1986).

16. J. L. Persson, R. L. Whetten, H.-P. Cheng and R. S. Berry, Chem. Phys. Lett. **186**, 215 (1991).

17. H. L. Davis, D.J. Wales and R. S. Berry, J. Chem. Phys. **92**, 4308 (1990).

18. R. S. Berry, P. Braier, R. J. Hinde and H.-P. Cheng, Israel J. Chem. **30**, 39 (1990); R. S. Berry, H.-P. Cheng and J. Rose, Proc. Sixth Int. Conf. on High Temperatures, April, 1989; National Institute for Science and Technology: Gaithersburg, Md.

19. J. Bernholc, J.-Y. Yi, and D. J. Sullivan, Faraday Society Discussions **92**, in press (1992).

20. J. Bernholc, J.-Y. Yi, Q.-M. Zhang, D. J. Sullivan, C. J. Brabec, S. A. Kajihara, E. B. Anderson, and B. N. Davidson, Proc. Intern. Symp. on the Physics and Chemistry of

Finite Systems - From Clusters to Crystals, edited by P. Jena, S. N. Khanna, and B. K. Rao, Kluver Academic, in press (1992).

21. Q. Zhang, J.-Y. Yi, and J. Bernholc, Phys. Rev. Lett. **66**, 2633 (1991).

22. V. P. Skripov, V. P. Koverda and V. N. Skokov, Phys. Stat. Sol. (a) **66**, 109 (1981).

23. R. S. Berry, J. Jellinek and G. Natanson, Phys. Rev. A **30**, 919 (1984).

24. R. S. Berry and D. J. Wales, Phys. Rev. Lett. **63**, 1156 (1989); D. J. Wales and R. S. Berry, J. Chem. Phys. **92**, 4473 (1990).

25. D. J. Wales and R. S. Berry, J. Chem. Phys. **92**, 4283 (1990).

26. H.-P. Cheng and R. S. Berry, Phys. Rev. A 45, 1 June (1992).

27. H.-P. Cheng, X. Li, R. L. Whetten and R. S. Berry, Phys. Rev. A, in press (1992).

28. T. P. Martin, Phys. Rep. **95**, 167 (1983).

29. J. Luo, U. Landman and J. Jortner, in *Physics and Chemistry of Small Clusters*, P. Jena, B. K. Rao and S. N. Khanna, eds. (Plenum, New York, 1987), p. 201.

30. J. P. Rose and R. S. Berry, J. Chem. Phys. **96**, 517 (1992).

31. C. A. Angell and K. J. Rao, J. Chem. Phys. **57**, 470 (1972); C. A. Angell and J. C. Tucker, J. Phys. Chem. **78**, 278 (1974), and refs. therein.

32. F. S. Howell, R. A. Bose, P. B. Macedo and C. T. Moynihan, J. Phys. Chem. **78**, 639 (1974) and refs. therein.

33. P. Salamon, J. Bernholc, R. S. Berry, M. E. Carrera-Patino and B. Andresen, J. Math. Phys. **31**, 610 (1990).

34. F. Amar, J. Bernholc, R. S. Berry, J. Jellinek and P. Salamon, J. Appl. Phys. **65**, 3219 (1989).

35. P. Basa, J. C. Schön, R. S. Berry, J. Bernholc, J. Jellinek, and P. Salamon, Physical Review B, **43**, 8113 (1991).

36. P. Basa, J. C. Schön and P. Salamon, in press, Quarterly of Applied Mathematics (1992).

37.   R. S. Berry, J. Bernholc and P. Salamon, Applied Physics Letters, 58, 595 (1991).

38. J. C. Schön and P. Salamon, submitted for publication, Physical Review B.

39. R. Frost, J. C. Schön, and P. Salamon, submitted for publication, SIAM Journal on Scientific and Statistical Computing.

40. P. Salamon, J. C. Schoen, R. Frost, and P. Basa, in <u>Clusters and Clustering: From Atoms to Fractals</u>, edited by P. Reynolds, North Holland, in print (1991).

41. J. C. Schoen and P. Salamon, in Clusters and Cluster-Assembled Materials, edited by R. S. Averback, J. Bernholc, and D. L. Nelson, MRS Symp. Proc. vol 206, p. 521 (1991).

42. J. C. Schön and P. Salamon, in press, Institute for Mathematics and its Applications proceedings, ed. J.C. Nietsche, Springer Verlag 1992.

43. T. Bejarano, "The Use of Dynamic Programming for the Wetting of Assemblies of Spheres and Disks," (M.S. Thesis, San Diego State University, Dept. of Math. Sciences, 1991).

44. R. M. German, *Liquid Phase Sintering* (Plenum Press, New York, 1985).

45. I. M. Lifshitz and V. V. Slyozow, J. Phys. Chem. Solids, **19**, 33 (1961).

46. J. C. Schön, R. Frost, M. Chu, J. Lawson and P. Salamon, to appear, J. App. Phys. (1992).